RSC Publishing Faraday Discussions

Poly(alkyl glycidyl ether) hydrogels for harnessing the bioactivity of engineered microbes

Journal:	*Faraday Discussions*
Manuscript ID	FD-ART-02-2019-000019.R1
Article Type:	Paper
Date Submitted by the Author:	04-Mar-2019
Complete List of Authors:	Johnston, Trevor; University of Washington System, Chemistry Fellin, Christopher; University of Washington, Chemistry Carignano, Alberto; University of Washington Nelson, Alshakim; University of Washington, Chemistry

ARTICLE

Poly(alkyl glycidyl ether) hydrogels for harnessing the bioactivity of engineered microbes

Received 00th January 20xx,
Accepted 00th January 20xx

DOI: 10.1039/x0xx00000x

Trevor G. Johnston,[a*] Christopher R. Fellin,[a*] Alberto Carignano,[b] Alshakim Nelson[a†]

Herein, we describe a method to produce yeast-laden hydrogel inks for direct-write 3D printing cuboidal lattices for immobilized whole-cell catalysis. A poly(alkyl glycidyl ether)-based triblock copolymer was designed to have three important features for this application: (1) a temperature response which allowed for facile processing of the material; (2) the shear response which facilitated the extrusion of the material through a nozzle; and (3) a UV-light induced polymerization which enabled the post extrusion chemical crosslinking of network chains, and the fabrication of robust printed objects. These three key stimuli responses were confirmed via rheometrical characterization. A genetically-engineered yeast strain with an upregulated α-factor production pathway was incorporated into the hydrogel ink and 3D printed. The immobilized yeast cells exhibited adequate viability of 87.5% within the hydrogel. The production of the up-regulated α-factor was detected using a detecting yeast strain and quantified at 268 nM (*s* = 34.6 nM) over 72 h. The reusability of these bioreactors was demonstrated by immersion of the yeast-laden hydrogel lattice in fresh SC media and confirmed by the detection of similar amounts of up-regulated α-factor 259 nM (s = 45.1 nM). These yeast-laden materials represent an attractive opportunity for whole-cell catalysis of other high-value products in a sustainable and continuous manner.

Introduction

Whole-cell biocatalysis is a standard practice across a wide range of industries wherein cells are used to transform molecular precursors into a product of interest (antibiotics, drugs, vitamins, insulin, vaccines, etc.). These reactions are generally employed as a batch process wherein the cells and the necessary molecular precursors are combined into a single reaction vessel, stirred for several days, and then the product is isolated from the complex mixture.[1–10] However, batch cell reactors are costly and time consuming because they require sterile conditions, can have low yields, and purification protocols are labor and cost intensive. Immobilized-cell bioreactors, wherein metabolically active cells are trapped within a material such as a hydrogel, offer an alternative method that can simplify the isolation of the product, minimize product inhibition or toxicity, and allow recycling of the cells.[11]

We have previously reported additive manufactured catalytically active living materials (AMCALM) as a platform for immobilized-cell bioreactors.[12] In contrast to previous reports wherein calcium alginate beads[13–16] or electrospun fibers[17–19] were used to encapsulate microbes for fermentation, our approach utilized customized lattices of yeast-laden hydrogels that were printed using a direct-write 3D printer. Additive manufacturing (or 3D printing) is a fabrication process that utilizes layer-by-layer material deposition to construct three-dimensional geometries according to a computer-aided design (CAD) model.[20–27] As such, 3D printing is well-suited for manufacturing living materials[28–33] with spatial and geometrical organization of cells. Hydrogel-based materials are particularly attractive as cell-laden inks for direct-write 3D printing because these materials can recapitulate some of the chemical and physical attributes of the extracellular matrix that exists in biofilms, living tissue, and other naturally occurring microenvironments.[31,34–36] These features could include the presence of ligands or functional groups,[37–40] or the stiffness of the hydrogel.[41,42]

There were three important features of the yeast-laden hydrogel ink that were developed for AMCALMs: (1) a temperature response, wherein the material exhibited a reversible gel-to-sol transition upon cooling, that enabled homogeneous dispersion of the yeast cells within the gel and facile loading of the hydrogel into a syringe; (2) a shear-thinning response that facilitated the extrusion of the hydrogel ink from a nozzle to enable the layer-by-layer formation of three-dimensional objects; and (3) an irreversible photo-response wherein polymerizable groups chemically cross-linked the hydrogel into a robust structure. Yeast-laden hydrogel lattices were printed and then utilized in a continuous batch process for the fermentation of glucose to produce ethanol.

Herein, we demonstrate a new polymer hydrogel for the encapsulation and direct-write 3D printing of yeast-laden hydrogel lattices that can be used for the production of a polypeptide. The poly(glycidyl ether)-based ABA triblock

[a.] *Department of Chemistry, University of Washington, Seattle, WA 98195*
[b.] *Department of Electrical Engineering, University of Washington, Seattle, WA 98195*
[*]These authors contributed equally to this work
[†]Correspondence to: Alshakim Nelson Department of Chemistry, University of Washington, Seattle, WA 98195. Email: alshakim@uw.edu

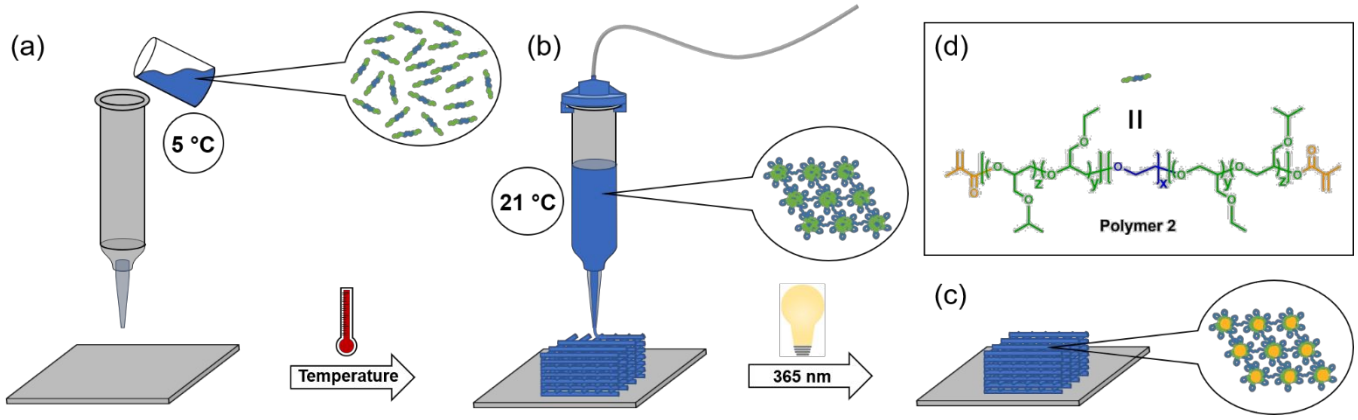

Figure 1. A graphical overview of the three key stimuli responses of polymer **2** hydrogels necessary for AMCALM applications. (a) The temperature responsive feature of the hydrogels enabled facile loading of the hydrogel material at 5 °C. (b) The shear-stress response facilitated the formation of complex three-dimensional objects at 21 °C. (c) UV-light (365 nm) initiated the polymerization of the methacrylate end-groups and chemical crosslinking of the polymer **2** hydrogel. (d) The chemical structure of polymer 2. The letter designations (z = 6.4, y = 7.4, x = 182) refer to the average number of isopropyl glycidyl ether, ethyl glycidyl ether, and ethylene oxide repeat units, respectively.

copolymer (polymer **2**) has similar features (temperature-, shear-, and photo-responses, Figure 1) to the Pluronic-based triblock copolymer that was reported previously.[12] Furthermore, a genetically-engineered yeast strain with an upregulated α-factor production pathway was incorporated into the hydrogel to demonstrate the production of an extracellularly excreted polypeptide from the yeast-laden hydrogel. While α-factor is a yeast hormone that does not have any known therapeutic effects, the polypeptide is commonly utilized in the expression and recovery of recombinant proteins.[43,44] When the α-factor leader sequence is appended to the genetic code for an engineered protein, the yeast cell utilizes its native cellular machinery to secrete the protein beyond the cell membrane.[45–50] In our experiments, we not only demonstrate that the secreted α-factor can be detected in the liquid media surrounding the hydrogel lattice, but also the reusability of the yeast-laden hydrogel lattices.

Experimental

Materials

All chemicals and solvents were purchased from Sigma-Aldrich or Fisher Scientific and used without further purification unless noted otherwise. Isopropyl glycidyl ether (iPGE, 98%) and ethyl glycidyl ether (EGE, 98%) were dried over CaH_2 for 24 h, distilled into a flask containing butyl magnesium chloride (2 M in tetrahydrofuran, THF), re-distilled, and stored under N_2 atmosphere. Poly(ethylene oxide) (PEO, M_n 8000 g mol^{-1}) was dried under vacuum overnight prior to use. Dry THF was obtained using neutral alumina using a Pure Process Technology solvent purification system. A potassium naphthalenide solution (1M) was prepared by dissolving naphthalene (3.2 g) in THF (25 mL), adding potassium (0.975 g), and storing under N_2 atmosphere. ^{1}H NMR spectra were obtained on a Bruker Advance 300 or 500 MHz spectrometer. Gel permeation chromatography was performed using a Waters chromatograph equipped with two 10 µm Malvern columns (300 mm x 7.8 mm) connected in series with increasing pore size (1,000, 10,000 Å), using chloroform (Optima, 0.1% v/v trimethylamine) as the eluent, and calibrated with poly(ethylene oxide) standards (400 to 40, 000 g mol^{-1}). The relative molecular weights were measured in chloroform using poly(ethylene oxide) standards and a refractive index detector (flow rate: 1 mL min^{-1}). Drop-out Mix Complete without Yeast Nitrogen Base D9515) and Yeast Nitrogen Base (Y2025) were purchased from US Biological Life Sciences. Sytox Green nucleic acid strain (5 mM solution in DMSO; Invitrogen) was purchased from Thermo Fisher Scientific.

Yeast Strains

For microscopy and live/dead viability tests, the strain yJS001 was used (genotype SO992 mfa2::pTEF1_mCherry(kanR)). This strain constitutively expressed mCherry protein, which facilitated characterization using fluorescence microscopy. *Saccharomyces cerevisiae* strain SO992 was used as the control strain in the α-factor production experiments. This strain is a derivative of W303 (genotype MATa ura3 leu2 trp1 his3 can1R ade).

As the α factor-producing strain, we employed a genetically modified MAT-α yeast strain ('secreting strain') expressing the *S. cerevisiae* gene MFα1 (YPL187W) on a constitutively-expressed promoter pGPD (natively expressing YPL197W). The MFα1 gene expresses 3 copies of the α-factor peptide, a 13-amino acid peptide natively used as mating hormone from the MAT-α to the MAT-A strains.

To quantify the α-factor secreted from the yeast immobilized in the hydrogels, we employed a genetically modified MAT-A yeast strain that expresses the fluorescence protein yeVenus driven by the pFUS1 promoter, which is downstream the MAPK signaling pathway, activated by α-factor detection ('detecting strain'). The MAT-A native strain was engineered by deleting BAR1 (native α-factor protease) and integrating the POG1 gene on a constitutively-expressed pGPD promoter to avoid α-factor-induced growth arrest.

Yeast transformations were carried out using a standard lithium acetate protocol. Yeast cells were made competent by growing 50 mL cultures in rich media to log growth phase, then spinning down the cells and washing with H20. Next, linearized DNA, salmon sperm donor DNA, 50% polyethylene glycol and

1M LiOAc were combined with 50 mL of competent cells and the mixture was heat shocked at 42 °C for 15 min. The cells were then spun down, supernatant was removed, and they were resuspended in H2O and then plated on selective agar media. Transformations were done into MATa W303-1A and MATα W303-1B background strains.

Synthesis of Polymer 1

The ABA triblock copolymer was synthesized via anionic ring-opening polymerization. PEO (M_n = 8,000 g mol^{-1}, 20 g, 2.5 mmol) was added to the reaction vessel and dried under vacuum overnight. Dry THF (250 mL) was added under an Ar atmosphere and heated to 50 °C to facilitate dissolution of the macroinitiator. Once sufficiently dissolved, a potassium naphthalenide solution (1M in THF) was titrated into the flask until the solution remained a slight green color, indicating full deprotonation of PEO hydroxyl end groups. Isopropyl glycidyl ether (4.94 g, 42.5 mmol) and ethyl glycidyl ether (4.34 g, 42.5 mmol) were added to begin polymerization. The reaction continued for 24 h at 65 °C and was subsequently quenched with a degassed solution of 1% v/v AcOH in MeOH. The reaction mixture was then precipitated into cold hexane. The polymer was collected via centrifugation (4400 rpm, 10 min) and the supernatant decanted. The product was washed twice with additional hexane and collected again in the same manner. The isolated polymer solution was dried in a vacuum oven for at least 24 h to afford polymer **1** as an off-white solid (27.5 g). ^{1}H NMR (500 MHz, $CDCl_3$): δ = 1.15-1.17 (m, -O-CH-(C$\underline{H}_3$)$_2$), 1.17-1.23 (t, -O-CH$_2$-C$\underline{H}_3$, J = 7.0 Hz), 3.47-3.81 (m -O-C$\underline{H}_2$-C$\underline{H}_2$-O- and -O-C$\underline{H}_2$-C$\underline{H}$(C$\underline{H}_2$-O-C$\underline{H}_2$-CH$_3$)-O- and -O-C$\underline{H}_2$-C$\underline{H}$(C$\underline{H}_2$-O-C$\underline{H}$-(CH$_3$)$_2$)-O-).

Synthesis of Polymer 2

Polymer **1** (20g, 1.81 mmol) was dissolved in dry THF (250 mL) under a nitrogen atmosphere until complete dissolution of the polymer. Triethylamine (2.45 mL, 18.1 mmol) was added to increase the reactivity of the polymer hydroxyl chain ends and the mixture was heated at 65 °C for 30 min. Methacrylic anhydride (26.9 mL, 181 mmol) was then added and the reaction mixture was stirred for 16 h at 65 °C. After this time, the reaction was quenched with a degassed solution of 1% v/v AcOH in MeOH. The reaction mixture was then precipitated into cold ether. The polymer was collected via centrifugation (4400 rpm, 10 min) and the supernatant decanted. The product was washed twice with additional ether, once with hexane, and collected again by centrifugation. The isolated polymer was dried in a vacuum oven for 24 h to afford polymer **2** as an off-white solid (16.7g). The degree of functionalization (f_n) was determined by comparing the integrations of the methacrylate vinyl (6.12 and 5.55 ppm) and methyl (1.94 ppm) protons, as well as the PEO chain-end methylene protons (5.08-5.15 ppm), to their theoretical values. For example, 1.99 (vinyl, actual)/2 (vinyl, theoretical) X 100 ≈ 100% functionalization of chain ends. These integration values were referenced to the total alkyl glycidyl ether protons for each polymer chain (1.12-1.20 ppm, 121 H). ^{1}H NMR (300 MHz, $CDCl_3$): δ = 1.12-1.20 (m, -O-CH-(C$\underline{H}_3$)$_2$) and -O-CH$_2$-C$\underline{H}_3$), 1.94 (s, C$\underline{H}_3$C(CO$_2$)=CH$_2$), 3.39-3.89 (m, -O-C$\underline{H}_2$-C$\underline{H}_2$-O- and -O-C$\underline{H}_2$-C$\underline{H}$(C$\underline{H}_2$-O-C$\underline{H}_2$-CH$_3$)-O-, and -O-C$\underline{H}_2$-C$\underline{H}$(C$\underline{H}_2$-O-C$\underline{H}$-(CH$_3$)$_2$)-O-), 5.08-5.15 (m, -CH$_2$-C$\underline{H}$-O-(C=O)), 5.48 (s, $\underline{H}$-CH=C), 6.18 (s, $\underline{H}$-CH=C).

Preparation of Synthetic Complete Media

The SC media (1L) was prepared by dissolving drop-out mix (2 g), yeast nitrogen base (6.7 g), and glucose (20 g) in Milli-Q water. The resulting solution was sterilized by filtration through a 0.2 μm nylon filter.

Preparation of Hydrogel Solution

Polymer **2** was dissolved in sterile, deionized water at a concentration of 20 wt % polymer. The resulting polymer solution was cooled overnight at 5 °C to facilitate hydrogel formation via LCST behavior. After homogenization of the solution at low temperature, the solution was warmed to 21 °C to induce the formation of a gel state. Hydrogels used to print the proof-of-concept models in Figure 3 were mixed with the photo-radical initiator 2-hydroxy-2-methylpropiophenone (10 μL) and centrifuged (4400 rpm, 10 min) to remove bubbles.

Preparation of Yeast-Laden Hydrogel ink

To prepare yeast-laden hydrogels, the aforementioned hydrogel solution was cooled to 5 °C in a refrigerator. At this temperature, the hydrogel solution underwent gel-to-sol transition, affording a free-flowing liquid. Yeast cells were added from an overnight liquid culture, at a concentration of 10^7 cells per gram of hydrogel while the gel was in its solution state. The resulting solution was mixed thoroughly and allowed to equilibrate at 5 °C until all of the bubbles present in the solution were removed. Finally, the hydrogel was warmed to 21 °C to undergo a sol to gel transition, resulting in a shear-responsive gel.

Rheometrical Characterization

For rheometrical characterization of the hydrogels, dynamic oscillatory experiments were performed on a TA Instruments Discovery Hybrid Rheometer-2 (DHR-2) equipped with a Peltier temperature controller. The instrument operates by applying a known displacement (strain) and measuring the material's resistance (stress) to the force. Rheometry experiments were conducted by depositing hydrogel between the rheometer base plate and 20 mm parallel plate geometry with a final gap of 1 mm. Samples were equilibrated in an ice bath for at least 30 min and then were carefully loaded onto the Peltier plate at 5 °C and a preshear experiment was applied to eliminate the bubbles from the sample. The sample was equilibrated at 21 °C for 8 min before each run. The gel yield stress values were measured under oscillatory strain (frequency: 1 Hz, 21 °C) starting with an initial strain of 0.01% and converted to applied oscillatory stress. Viscosity versus shear rate experiments were performed in the range of shear rates between 0.01 and 100 Hz. Cyclic shear thinning experiments (frequency = 1 Hz) were performed at 21 °C using alternating strains of 1% for 5 min and 100% for 3 min per cycle, to investigate the shear-thinning and recovery behavior of the hydrogels. Temperature ramp experiments were performed at 1 Hz from 5−50 °C at 2 °C min^{-1}. Photocuring

was performed using a fully integrated smart swap LED photo curing accessory. A 120 s dwell time (frequency: 1 Hz) elapsed before the UV lamp (365 nm LED with an irradiation intensity of 5 mW cm^{-2}) was turned on for 420 s at a constant oscillatory strain (1%).

Additive Manufacturing (Direct-Write 3D Printing) of a Cuboidal-Lattice

A modified pneumatic direct-write 3D printer was assembled based on a Tronxy P802E 3D Printer kit, from Shenzen Tronxy Technology Co. The printer was controlled with an Arduino using the Marlin firmware. All CAD models were designed in OpenSCAD. G-code commands for the printer were generated using Slic3r. The resulting G-code was modified using Python to introduce required commands for the dispensing of the hydrogel via pneumatic pressure. All printing was performed using a 20 wt % hydrogel ink with an extrusion air pressure of 20 psi, a print speed of 5 mm s^{-1}, and a 0.41 mm inner diameter CML Supply conical nozzle attachment.

The dimensions for the 3D printed lattices are 1.9 cm by 1.9 cm by 1.2 cm and each cube weighed between 1.8 and 2.0 g. Upon completion of the 3D printing, the cubes were irradiated under 365 nm light (at 3.4 mW cm^{-2}) for 3 min to cure and chemically fix the structures.

Microscopy and Imaging

Optical imaging: Images of the 3D-printed hydrogels were captured using an iPhone XS. Confocal imaging: Confocal microscopy images were taken using a Leica TCS SP5 II laser scanning confocal microscope. All images were taken with a dry 20x objective. MCherry protein fluorescence was excited with a 561 nm laser at 5% laser power, and emission was scanned from 569 to 700 nm. Sytox green viability dye was excited with a 488 nm laser at 5% laser power, and emission was scanned from 500 to 550 nm. Samples were sequentially scanned, and the output images were processed using ImageJ Java software.

Cell Viability Assay

The yeast-laden hydrogel was prepared as described above. This gel was cooled to 5 °C to induce a gel-to-sol transition, which was then poured and spread into a sterile petri dish to produce a thin film (~0.5 mm) of the yeast-laden hydrogel. The sample was irradiated with 365 nm UV light for 3 min. This film was then incubated in fresh SC media at 30 °C, and periodically agitated. The media was exchanged every 24 h to ensure fresh nutrient delivery to the embedded cells. At the imaging intervals described in this work, a small square of the film (5 mm × 5 mm) was cut and removed for staining. Sytox Green stain stock solution was diluted to 5 µM, and 20 µL of the dye solution was exposed to hydrogel sample for 5 min. The sample was then washed with SC media and imaged using a Leica SP5 confocal microscope. Constitutively expressed mCherry protein fluorescence from the yeast cells was measured to indicate live cells, while the Sytox dye fluorescence indicated the presence of dead cells.

α-Factor Production

α-Factor production from 3D printed yeast-laden cuboidal lattices was quantified as follows. A yeast-laden hydrogel ink containing 10^7 yeast cells per gram of hydrogel was direct-write 3D printed and photo-cured (3 min) with 365 nm irradiation. The lattices were then washed with SC media, and placed into 50 mL falcon tubes. The tubes were then filled with 10 mL of SC media for fermentation and placed in a 30 °C shaker (225 rpm) for incubation. After a period of 72 h, the lattices were removed from the reactors and the media was collected. The fermentation media was filtered with a 0.2 µm nylon filter. The up-regulated yeast strain experiments were performed in triplicate alongside a wild-type yeast-laden lattice.

To determine the reusability of the lattices in subsequent fermentation cycles, the same lattices from the first round of α-factor were again washed individually in sterile SC media. The lattices were then placed into new falcon tubes containing 10 mL of SC media, and incubated at the same conditions for an additional 72 h. After incubation, the samples were collected and prepared for characterization in the same manner as mentioned above.

α-Factor Detection and Quantification

To quantify α-factor synthesis from within the yeast-laden hydrogel, we collected the SC media that was used to submerge the hydrogel sample after 72 h. We collected 9 mL of media for each experimental condition and replicate; each sample was split into six 1.5 mL Eppendorf tube and then dehydrated in a Savant SpeedVac Plus SC110A Concentrator for 12 h at Medium dehydration speed. Subsequently, we added 100 µL of molecular graded water into each dehydrated sample, resuspended, and collected the resulting 600 µL into a single sample. The final sample was run again through the Speed-Vac for 12 h at Medium speed and resuspended into 100 µL of molecular graded water. This process concentrated the initial sample to 90-fold its original concentration.

We experimentally tested for α-factor synthesis using detecting strains with a standard cytometer assay protocol. The detecting strains were grown overnight for 20 h in SC media, then diluted to 30 events/µL again in SC media. After 3 h, we inoculated the concentrated samples from the yeast-laden hydrogels into different vials, plus two extra vials: one kept as control (3 µL of 0.1 M Sodium Acetate) and one was inoculated with 10 µM 98% HPLC-pure α-factor peptide in 0.1 M Sodium Acetate obtained from Zymo Research (Irvine, CA, USA). Samples were collected for cytometer measurement 8 h after induction, and median fluorescence values were computed from the resulting histogram.

Fluorescence intensity of the detecting strain was measured with a BD Accuri C6 flow cytometer equipped with a CSampler plate adapter using excitation wavelengths of 488 and 640 nm and an emission detection filter at 533 nm (FL1 channel). A total of 10,000 events above a 400,000 FSC-H threshold (to exclude debris) were recorded for each sample with and core size of 22 mm using the Accuri C6 CFlow Sampler software. Cytometry data were exported as FCS 3.0 files and processed using custom Python scripts to obtain the median FL1-A value at each data point.

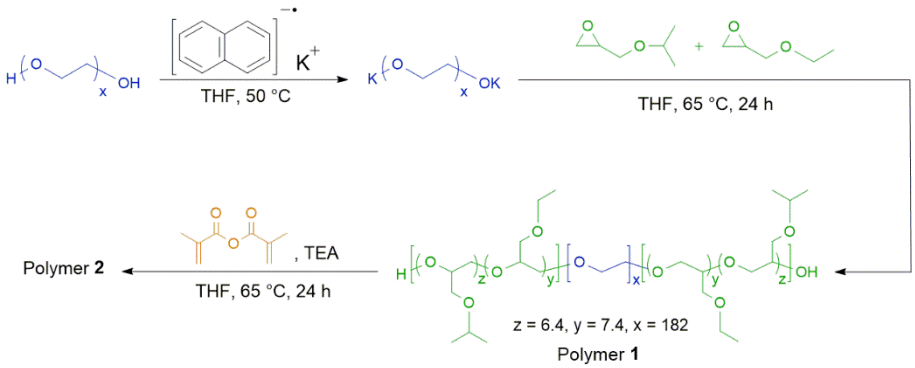

Scheme 1. Synthesis of the ABA triblock copolymer (polymer **1**) and functionalization with methacrylic anhydride (polymer **2**). The letter designations (z = 6.4, y = 7.4, x = 182) refer to degree of polymerization for isopropyl glycidyl ether, ethyl glycidyl ether, and ethylene oxide, respectively.

We used a model fitted to data to estimate the amount of α-factor detected by the detecting strain starting from its median fluorescence value response. The model interpolates a titration curve of an α-factor-detecting strain that is equivalent to the one used in this study, except its synthesis yeGFP fluorescent protein instead of yeVenus. The interpolation follows a standard Hill activation function:

$$y = K\frac{u^n}{\varphi + u^n} + y_0$$

where *u* represents the α-factor input concentration in nM, and *y* the median fluorescence output. To account for the different fluorescent protein, we used the control and the 10 μM α-factor median fluorescent outputs from this experiment to re-fit K and y_0.

To estimate the amount of α-factor synthesized by our strains in the hydrogel, we inverted the formula above to get:

$$u = \sqrt[n]{\varphi\frac{y - y_0}{K + y_0 - y}}$$

Results and Discussion

Synthesis and Functionalization of the Triblock Copolymer.

ABA triblock copolymers of poly(isopropyl glycidyl ether-*stat*-ethyl glycidyl ether)-*block*-poly(ethylene oxide)-*block*-poly(isopropyl glycidyl ether-*stat*-ethyl glycidyl ether) afford shear-thinning hydrogels that have a tunable sol-gel transition temperature based on the ratio of ethyl and isopropyl glycidyl ether monomers (EGE and iPGE, respectively), 'A' block chain length, and concentration.[51] When these polymers were dissolved in aqueous media, flower-like micelles[52] were expected to form based on the design of this ABA triblock copolymer--hydrophobic 'A' blocks flanking a hydrophilic 'B' block. Hydrogels based on this ABA triblock copolymer platform (20 wt%) were suitable inks for direct-write 3D printing and were able to create self-supporting hydrogel structures.[52] However, the physical cross-links present in this system were insufficient to maintain the integrity of the 3D printed object when subjected to either excess aqueous media or to mechanical loads. Thus, chemically cross-linked hydrogels are necessary to improve the robustness of the 3D printed objects.

Polymer **1** was synthesized (Scheme 1) via living anionic ring-opening polymerization[53–56] from a poly(ethylene oxide) (PEO) macroinitiator (M_n = 8,000 g mol^{-1}) with an EGE:iPGE ratio of 1.15:1 to afford triblock copolymers with narrow dispersity (Đ = 1.11). Polymerizable methacrylate groups were introduced onto the chain-ends of polymer **1** to afford polymer **2** (Scheme 1). We hypothesized that the resulting polymer hydrogel would maintain its thermal- and shear-responses pre-extrusion, and then photochemically cross-link post-extrusion. The degree of chain-end functionalization (f_n) was determined by comparing the integrations of the methacrylate vinyl (6.12 and 5.55 ppm) and methyl (1.94 ppm) protons, as well as the PEO chain-end methylene protons (5.08-5.15 ppm), to their theoretical values and was found to be quantitative. The polymer was dissolved water (20 wt %) and 2-hydroxy-2-methylpropiophenone was added as the photo-radical initiator (0.1 wt%) for polymerization of the methacrylate groups.

Rheology of the Functionalized Triblock Copolymer Hydrogel.

The viscoelastic properties of a 20 wt% solution of polymer **2** in water were characterized using a rheometer. The temperature-dependent viscoelastic behavior of the gel was confirmed by the presence of a sol-gel transition as defined by the intersection of the elastic (G') and viscous (G") moduli (15.61 °C, Figure 2a). The solution maintained a non-viscous, liquid-like morphology at 5 °C and became a self-supporting hydrogel network by 21 °C. The temperature-dependent sol-gel transition was also confirmed visually as shown in the photographs in Figure S1.

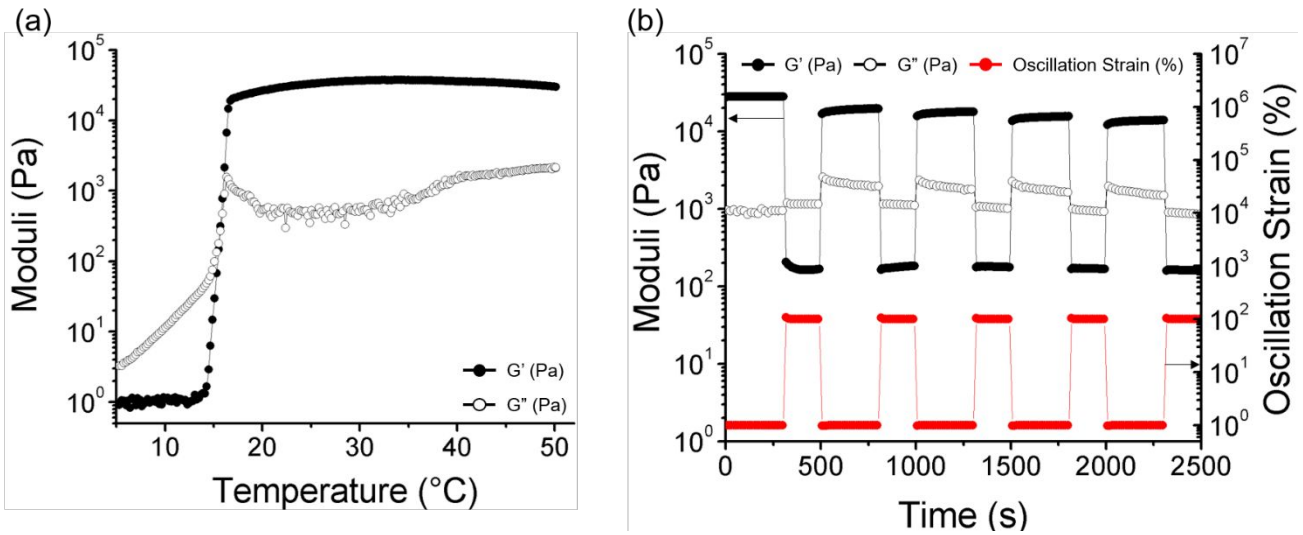

Figure 3. Rheometrical experiments for a 20 wt% formulation of polymer **2**. (a) Dynamic oscillatory temperature ramp displaying elastic (G', filled) and viscous (G'', open) moduli. T_{gel} = 15.61 °C. (b) Cyclic strain experiment demonstrating rapid recovery of hydrogel elastic modulus (black circles) from periods of high (100%) to low (1%) oscillatory strain (red circles). Arrows indicate reference axis; elastic/viscous moduli (left axis) and oscillatory strain (right axis).

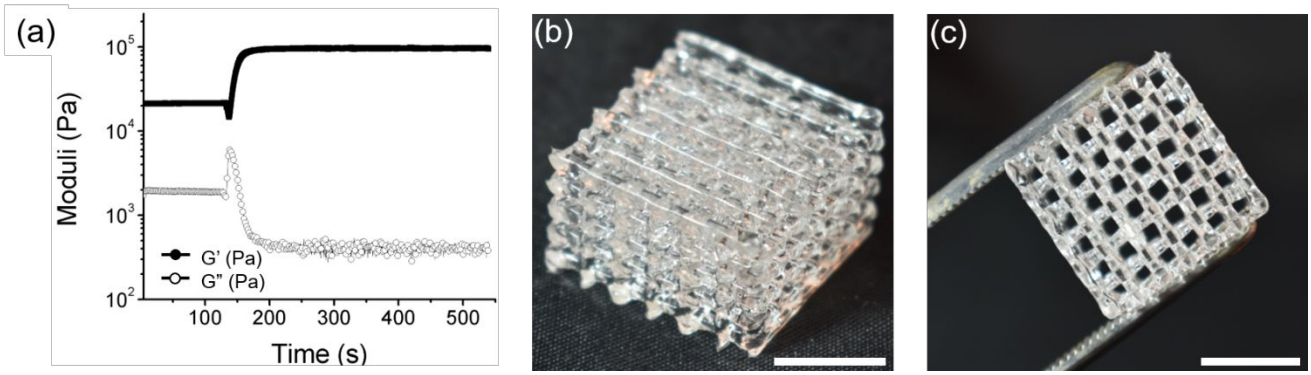

Figure 2. (a) A rheological UV-cure experiment using a 20 mm parallel plate geometry. The hydrogel was equilibrated for 120 s before being subjected to 5 mW cm-2 of 365 nm UV light for 420 s at a constant strain (1%) and frequency (1 Hz). (b-c) A 3D printed, proof of concept cuboid structure (1.9 cm by 1.9 cm by 1.2 cm). This structure was printed from a pneumatic direct write 3D printer at 5 mm s-1 and 20 psi using a 0.41 mm inner diameter nozzle (scale bar: 1 cm).

Hydrogels based on polymer **2** also exhibited shear-thinning behavior. The viscosity of the material decreased with increasing applied shear rate, which is indicative of a shear thinning hydrogel. An oscillatory strain sweep experiment afforded a yield stress value of 1.33 kPa (Figure S2-3). A dynamic oscillatory strain experiment (Figure 2b) demonstrated the strain dependent viscoelastic behavior of the gel upon repeated cycles of high (100%) and low (1%) strain. Initially under low strain, the material exhibited a gel-like morphology as indicated by greater values for G' relative to G". During periods of high strain, G" exceeded G', which indicated that the gel had a higher viscous character consistent with the material in its sol state. The material rapidly recovered to its gel state when the strain was reduced to 1% and exhibited very little mechanical hysteresis.

The post-extrusion UV cure of the gel was simulated under constant strain (1%) and frequency (1 Hz). After 120 s of equilibration time, the hydrogel was subjected to 5 mW cm^{-2} of 365 nm UV light for 420 s. The G' of the hydrogel increased from 21.56 kPa to 94.23 kPa within 75 s of UV exposure, and the G" decreased from 1.88 kPa to 0.47 kPa in the same time frame. These changes to the G' and G" were indicative of a rapid chemical crosslinking of the hydrogel network via photo-induced radical polymerization of the methacrylated chain ends (Figure 3a).

Direct-Write 3D Printing of Triblock Copolymer Dimethacrylate Hydrogels.

Utilizing these three stimuli responses, a proof of concept cuboidal lattice was 3D printed using a pneumatic direct write 3D printer at 5 mm s^{-1} and 20 psi with a 0.41 mm inner diameter conical nozzle. The temperature response allowed for facile processing of the hydrogel into the syringe at 5 °C in its liquid state. The hydrogel was then warmed to ambient temperature and extruded. The shear-response facilitated the extrusion of the hydrogel as rod-like filaments. A cuboidal lattice structure, with dimensions of 1.9 cm by 1.9 cm by 1.2 cm, was cured post-extrusion using a custom-made UV box equipped with two 365 nm A19 UV lamps for 180 s at 3.4 mW cm^{-2} (Figure 3b-c). The cuboidal lattice structure was chosen to simultaneously demonstrate a high-surface-area structure that promotes media circulation around the bioreactor in application, while

also demonstrating the structural integrity of the printed filaments that span unsupported overhangs.

Incorporation of Yeast Cells and Cell Viability

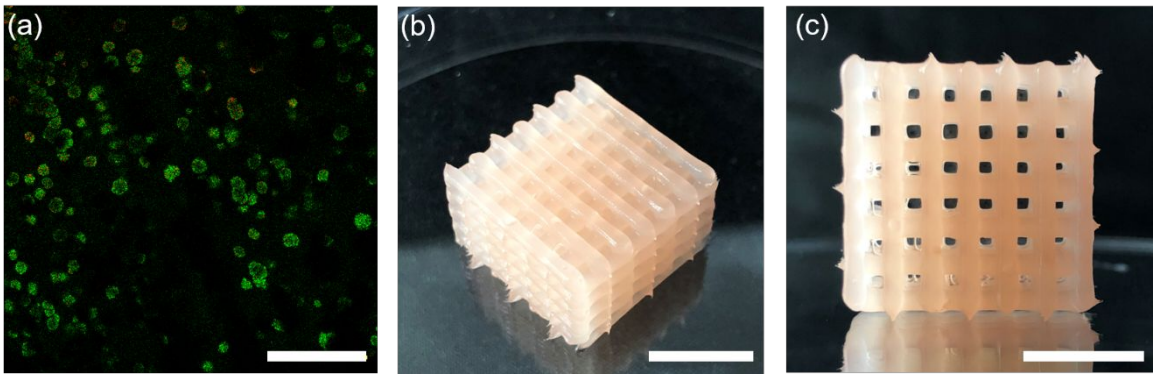

Figure 4. (a) A sample composite image of live cells (green channel) and dead cells (red channel) after 7 days of incubation (scale bar: 200 µm). (b) Side and (c) top-down view of the 3D-printed, yeast-laden hydrogel after two rounds of α-factor synthesis in SC media (scale bar 1 cm).

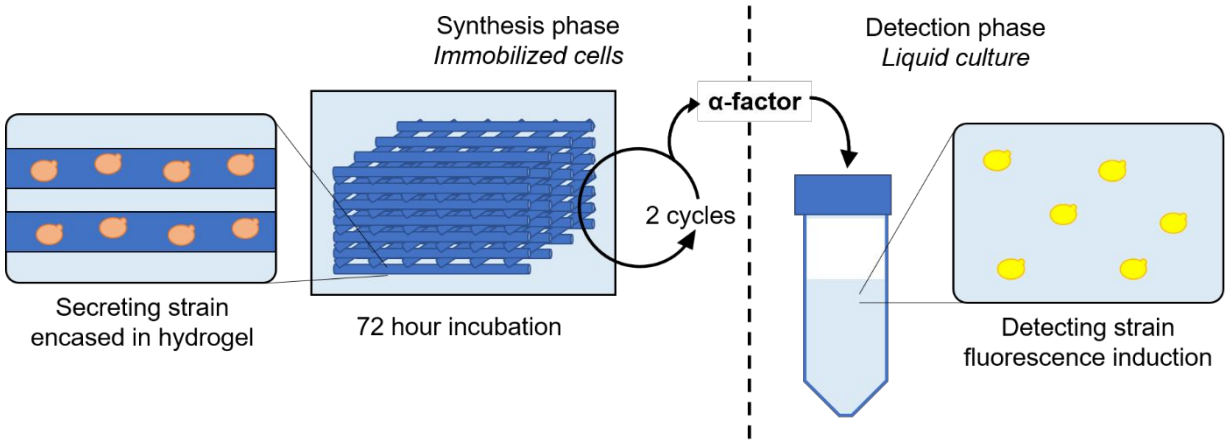

Figure 4. Immobilized yeast within the hydrogel matrix were incubated in SC media for 72 h at 30 °C with automated shaker agitation. The media was collected at the end of the incubation period and exposed to the receiver strain in a separate tube, and the resulting fluorescence was measured. The cuboidal lattice was reused in a subsequent incubation with fresh media to produce an additional batch of α-factor.

To ensure the viability of encapsulated yeast cells within the polymer **2** hydrogel, *Saccharomyces cerevisiae* constitutively expressing mCherry fluorescent protein was inoculated into a solution of polymer **2** at 5 °C and mixed to make a homogenous mixture. A film of the resulting yeast-laden solution was cast at the same temperature, subsequently warmed to 21 °C to induce gelation, and cured to create a physically robust hydrogel film. This yeast-laden film appeared transparent after processing due to the relatively low loading concentration of yeast cells. A small sample of the yeast-laden hydrogel film was extracted, stained, and imaged periodically over seven days. Sytox green staining results showed that cells remained 87.5% viable within the cast hydrogel at the end of the week of imaging, as seen in Figures 4a and Figures S4-S6. Significant cell colony growth was observed by both confocal microscopy and optical imaging. This growth was also observed visually, as indicated by the opacity of the 3D-printed hydrogel structure in Figure 4b-c. These results suggest that the poly(alkyl glycidyl ether)-based hydrogels are comparable in their ability to house and promote yeast cell viability over time to our previously employed[12] F127-based hydrogels.

α-Factor Production with 3D Printed AMCALMs

An engineered yeast strain with upregulated α-factor production was used to demonstrate AMCALM lattices that produced a polypeptide. The pGPD promoter present in the secreting yeast strain allowed the constitutive expression of the MFα1 gene, and thus, continuous production of the α-factor polypeptide. After the reaction, the aqueous reaction media was exposed to the detecting strain that fluoresced in the presence of α-factor.

These lattices were incubated in SC media for a period of 72 h (Figure 5), producing an average of 268 nM (s = 34.6 nM) of α-factor (Figure 6). The induced fluorescence response from the cuboidal lattice with the secreting strain was 4.40 times greater that of the control strain cuboidal lattice (without upregulated α-factor), which indicated that the up-regulation of the α-factor pathway was successful in the secreting strain. These results provide evidence that AMCALMs were suitable for the production of polypeptides, and that the products could readily diffuse out from the hydrogel matrix into the surrounding media.

One advantage of using an immobilized yeast platform for polypeptide synthesis is the potential to reuse the printed cuboidal lattices. We investigated the reusability of the poly(alkyl glycidyl ether)-based hydrogel living materials for the

continued production of α-factor in subsequent batch reactions. When the printed AMCALMs were removed from their first 72 h incubation, and placed into fresh media, they continued to produce an average of 259 nM (s = 45.1 nM) of α-factor after a second 72 h cycle (Figure 6). The second batch production was directly comparable to the output achieved during the first batch reaction, which suggests that these immobilized cell bioreactors could be useful for continuous whole-cell catalysis.

Conclusion

In conclusion, we developed an ABA triblock copolymer based on a poly(alkyl glycidyl ether) that is suitable for 3D printing yeast-laden hydrogels for whole-cell catalysis. These polymer hydrogels exhibit a temperature, shear, and UV-light responsive behaviors that are integral to the preparation of the hydrogel ink and subsequent printing. The post-extrusion, chemical crosslinking of the polymer micelles induced by UV-light is particularly important to fabricate robust forms that do not degrade or dissolve over time.

The poly(alkyl glycidyl ether) based hydrogels also proved to have a negligible effect on the viability and biological activity of the encapsulated yeast cells. The engineered yeast-laden living materials were shown to be capable of producing an average of 263.5 nM of α-factor during two consecutive batch reactions, exhibiting no significant reduction in efficiency between the two cycles.

In this work, we demonstrated that polypeptides can be produced using the AMCALM platform. This result, combined with the prominence of the α-factor leader sequence in recombinant protein design and production, suggests that that these materials could be employed in the whole-cell catalysis of other higher-value molecules in a sustainable and continuous manner.

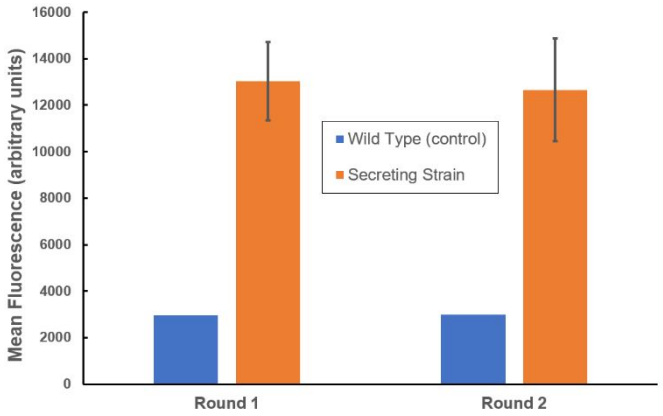

Figure 6. Fluorescence values obtained from the quantification of α-factor produced from the wild type (control) AMCALMs and the secreting strain AMCALMs. Round 1 indicates the first incubation period of 72 h, while Round 2 indicates the reemployment of the same printed materials in a second, subsequent 72 h batch reaction in fresh SC media.

Acknowledgements

The authors thank Dr. Eric Klavins of the University of Washington for continued consultation and expertise on yeast and biological systems. A.N. gratefully acknowledges support of this research by the National Science Foundation CAREER grant (DMR 1752972). This work was also partially funded by the Army Research Office (W911NF-17-1-0595). The authors thank The Biology Imaging Facility at the University of Washington for the use of the SP5 confocal microscope.

References

1 Y.-H. P. Zhang, J. Sun and Y. Ma, *J. Ind. Microbiol. Biotechnol.*, 2017, **44**, 773–784.
2 Y. Li and C. D. Smolke, *Nat. Commun.*, 2016, **7**, 12137.
3 K. Thodey, S. Galanie and C. D. Smolke, *Nat. Chem. Biol.*, 2014, **10**, 837–844.
4 A. R. Awan, B. A. Blount, D. J. Bell, W. M. Shaw, J. C. H. Ho, R. M. McKiernan and T. Ellis, *Nat. Commun.*, 2017, **8**, 15202.
5 T. U. Gerngross, *Nat. Biotechnol.*, 2004, **22**, 1409–1414.
6 C. J. Paddon, P. J. Westfall, D. J. Pitera, K. Benjamin, K. Fisher, D. McPhee, M. D. Leavell, A. Tai, A. Main, D. Eng, D. R. Polichuk, K. H. Teoh, D. W. Reed, T. Treynor, J. Lenihan, H. Jiang, M. Fleck, S. Bajad, G. Dang, D. Dengrove, D. Diola, G. Dorin, K. W. Ellens, S. Fickes, J. Galazzo, S. P. Gaucher, T. Geistlinger, R. Henry, M. Hepp, T. Horning, T. Iqbal, L. Kizer, B. Lieu, D. Melis, N. Moss, R. Regentin, S. Secrest, H. Tsuruta, R. Vazquez, L. F. Westblade, L. Xu, M. Yu, Y. Zhang, L. Zhao, J. Lievense, P. S. Covello, J. D. Keasling, K. K. Reiling, N. S. Renninger and J. D. Newman, *Nature*, 2013, **496**, 528–532.
7 W. C. DeLoache, Z. N. Russ, L. Narcross, A. M. Gonzales, V. J. J. Martin and J. E. Dueber, *Nat. Chem. Biol.*, 2015, **11**, 465–471.
8 S. Yang, Q. Fei, Y. Zhang, L. M. Contreras, S. M. Utturkar, S. D. Brown, M. E. Himmel and M. Zhang, *Microb. Biotechnol.*, 2016, **9**, 699–717.
9 A. M. Davy, H. F. Kildegaard and M. R. Andersen, *Cell Syst.*, 2017, **4**, 262–275.
10 P. P. Peralta-Yahya, F. Zhang, S. B. del Cardayre and J. D. Keasling, *Nature*, 2012, **488**, 320–328.
11 P. J. Verbelen, D. P. De Schutter, F. Delvaux, K. J. Verstrepen and F. R. Delvaux, *Biotechnol. Lett.*, 2006, **28**, 1515–1525.
12 A. Saha, T. G. Johnston, R. T. Shafranek, C. J. Goodman, J. G. Zalatan, D. W. Storti, M. A. Ganter and A. Nelson, *ACS Appl. Mater. Interfaces*, 2018, **10**, 13373–13380.
13 P. S. J. Cheetham, K. W. Blunt and C. Bocke, *Biotechnol. Bioeng.*, 1979, **21**, 2155–2168.
14 S. Nagarajan, A. L. Kruckeberg, K. H. Schmidt, E. Kroll, M. Hamilton, K. McInnerney, R. Summers, T. Taylor and F. Rosenzweig, *Proc. Natl. Acad. Sci.*, 2014, **111**, E1538–E1547.
15 B. A. E. Lehner, D. T. Schmieden and A. S. Meyer, *ACS Synth. Biol.*, 2017, **6**, 1124–1130.
16 A. Lode, F. Krujatz, S. Brüggemeier, M. Quade, K. Schütz, S.

Knaack, J. Weber, T. Bley and M. Gelinsky, *Eng. Life Sci.*, 2015, **15**, 177–183.
17 A. Townsend-Nicholson and S. N. Jayasinghe, *Biomacromolecules*, 2006, **7**, 3364–3369.
18 Y. Liu, M. H. Rafailovich, R. Malal, D. Cohn and D. Chidambaram, *Proc. Natl. Acad. Sci. U. S. A.*, 2009, **106**, 14201–14206.
19 I. Letnik, R. Avrahami, J. S. Rokem, A. Greiner, E. Zussman and C. Greenblatt, *Biomacromolecules*, 2015, **16**, 3322–3328.
20 A. Brimmo, P. A. Goyette, R. Alnemari, T. Gervais and M. A. Qasaimeh, *Sci. Rep.*, 2018, **8**, 10995.
21 T. Dahlberg, T. Stangner, H. Zhang, K. Wiklund, P. Lundberg, L. Edman and M. Andersson, *Sci. Rep.*, 2018, **8**, 3372.
22 S. Mamatha, P. Biswas, P. Ramavath, D. Das and R. Johnson, *Ceram. Int.*, 2018, **44**, 19278–19281.
23 R. Melnikova, A. Ehrmann and K. Finsterbusch, *IOP Conf. Ser. Mater. Sci. Eng.*, 2014, **62**, 012018.
24 M.-W. Sa, B.-N. B. Nguyen, R. A. Moriarty, T. Kamalitdinov, J. P. Fisher and J. Y. Kim, *Biotechnol. Bioeng.*, 2018, **115**, 989–999.
25 R. U. Kiran, S. Malferrari, A. Van Haver, F. Verstreken, S. N. Rath and D. M. Kalaskar, *Mater. Des.*, 2018, **162**, 263–270.
26 S. C. Ligon, R. Liska, J. Stampfl, M. Gurr and R. Mülhaupt, *Chem. Rev.*, 2017, **117**, 10212–10290.
27 M. J. Kimlinger and R. S. Martin, *Electroanalysis*, 2018, **30**, 2241–2249.
28 M. Müller, J. Becher, M. Schnabelrauch and M. Zenobi-Wong, *Biofabrication*, 2015, **7**, 035006.
29 L. E. Bertassoni, J. C. Cardoso, V. Manoharan, A. L. Cristino, N. S. Bhise, W. A. Araujo, P. Zorlutuna, N. E. Vrana, A. M. Ghaemmaghami, M. R. Dokmeci and A. Khademhosseini, *Biofabrication*, 2014, **6**, 024105.
30 Y.-C. Li, Y. S. Zhang, A. Akpek, S. R. Shin and A. Khademhosseini, *Biofabrication*, 2016, **9**, 012001.
31 S. Patra and V. Young, *Cell Biochem. Biophys.*, 2016, **74**, 93–98.
32 M. Schaffner, P. A. Rühs, F. Coulter, S. Kilcher and A. R. Studart, *Sci. Adv.*, 2017, **3**, eaao6804.
33 C. Bader, W. G. Patrick, D. Kolb, S. G. Hays, S. Keating, S. Sharma, D. Dikovsky, B. Belocon, J. C. Weaver, P. A. Silver and N. Oxman, *3D Print. Addit. Manuf.*, 2016, **3**, 79–89.
34 J. M. Lee and W. Y. Yeong, *Adv. Healthc. Mater.*, 2016, **5**, 2856–2865.
35 A. S. Hoffman, *Adv. Drug Deliv. Rev.*, 2002, **54**, 3–12.
36 K. Y. Lee and D. J. Mooney, *Chem. Rev.*, 2001, **101**, 1869–1880.
37 K. Smetana, *Biomaterials*, 1993, **14**, 1046–1050.
38 K. Smetana, J. Vacík, D. Součková, Z. Krčová and J. Šulc, *J. Biomed. Mater. Res.*, 1990, **24**, 463–470.
39 D. S. W. Benoit, M. P. Schwartz, A. R. Durney and K. S. Anseth, *Nat. Mater.*, 2008, **7**, 816–823.
40 J. H. Lee, H. W. Jung, I.-K. Kang and H. B. Lee, *Biomaterials*, 1994, **15**, 705–711.
41 D. E. Discher, P. Janmey and Y. L. Wang, *Science*, 2005, **310**, 1139–1143.
42 A. Buxboim, K. Rajagopal, A. E. X. Brown and D. E. Discher, *J. Phys. Condens. Matter*, 2010, **22**, 194116.
43 Z. Liu, K. E. J. Tyo, J. L. Martínez, D. Petranovic and J. Nielsen, *Biotechnol. Bioeng.*, 2012, **109**, 1259–1268.
44 T. Achstetter, *Mol. Cell. Biol.*, 1989, **9**, 4507–4514.
45 E. H. Baba and I. Berkower, *Biochem. Biophys. Res. Commun.*, 1992, **184**, 50–59.
46 J. A. Rakestraw, S. L. Sazinsky, A. Piatesi, E. Antipov and K. D. Wittrup, *Biotechnol. Bioeng.*, 2009, **103**, 1192–1201.
47 A. S. Robinson, V. Hines and K. D. Wittrup, *Nat. Biotechnol.*, 1994, **12**, 381–384.
48 J. Staniulis, *Biologija*, 2006, **3**, 49–53.
49 Y. Chigira, T. Oka, T. Okajima and Y. Jigami, *Glycobiology*, 2008, **18**, 303–314.
50 T. Kjeldsen, A. Frost Pettersson and M. Hach, *J. Biotechnol.*, 1999, **75**, 195–208.
51 C. R. Fellin, S. M. Adelmund, D. G. Karis, R. T. Shafranek, R. J. Ono, C. G. Martin, T. G. Johnston, C. A. DeForest and A. Nelson, *Polym. Int.*, 2018, DOI:10.1002/pi.5716.
52 M. A. Winnik and A. Yekta, *Curr. Opin. Colloid Interface Sci.*, 1997, **2**, 424–436.
53 B. F. Lee, M. J. Kade, J. A. Chute, N. Gupta, L. M. Campos, G. H. Fredrickson, E. J. Kramer, N. A. Lynd and C. J. Hawker, *J. Polym. Sci. Part A Polym. Chem.*, 2011, **49**, 4498–4504.
54 S. Heinen, S. Rackow, A. Schäfer and M. Weinhart, *Macromolecules*, 2017, **50**, 44–53.
55 Y. Satoh, K. Miyachi, H. Matsuno, T. Isono, K. Tajima, T. Kakuchi and T. Satoh, *Macromolecules*, 2016, **49**, 499–509.
56 K. P. Barteau, M. Wolffs, N. A. Lynd, G. H. Fredrickson, E. J. Kramer and C. J. Hawker, *Macromolecules*, 2013, **46**, 8988–8994.